Inorganic Chemistry

Article

pubs.acs.org/IC

New P2 Compound with Brucite-Like Layers: Potassium Lithiostannate

Igor L. Shukaev* and Vera V. Butova

Faculty of Chemistry, Southern Federal University, 7, ul. Zorge, Rostov-on-Don, 344090, Russia

Supporting Information

ABSTRACT: A new compound with brucite-like layers, $K_{0.72}Li_{0.24}Sn_{0.76}O_2$, has been obtained two ways, via solid-state reactions: with a big excess of KOH and in a controllable atmosphere without water and carbon dioxide. It has P2 structure (in Hagenmuller's definition) as previously described for $K_{0.70}Zn_{0.35}Sn_{0.65}O_2$. The latter compound has been repeatedly prepared using the new technique presented here. The structure was refined using powder X-ray profile analysis. Lithium cations are disordered with tin (+4) in the rigid part and introduce "acid" properties. Both types of potassium positions are split. The metastable P3 phase also appears in the $K_2O-Li_2O-SnO_2$ system. The sodium analogue $Na_{0.72}Li_{0.24}Sn_{0.76}O_2$ with P2 structure has been prepared using an ion-exchange technique.

1. INTRODUCTION

Structures with brucite-like layers possess a rather high potassium cationic conductivity (Table 1). Brucite-like layers consist of share edges octahedra. There are several types of structures, which differ from each other by the arrangement of layers. We use the following definitions:[6] letters represent the coordination of interlayer cations (O = octahedral, P = prismatic) and numbers represent the quantity of layers per unit cell. For example, structure types of α-$NaFeO_2$ and β-$RbScO_2$ are labeled as O3 and P2, respectively.

Table 1. Ionic Conductivity of Some Substances with Brucite-Like Layers

compound	structure type	temperature, T [K]	σ [Ω^{-1} m^{-1}]	ref
$Na_{0.8}Fe_{0.8}Ti_{0.2}O_2$	O3	573	0.6	1
$Na_{0.68}Mg_{0.68}Ti_{0.32}O_2$	O3	573	0.3	2
$K_{0.58}Zn_{0.29}Sn_{0.71}O_2$	P3	500	0.78	3
$K_{0.59}Mg_{0.53}Sb_{0.47}O_2$	P3	500	0.63	4
$K_{0.72}In_{0.72}Sn_{0.28}O_2$	P2	500	2.2	5
$K_{0.56}Ni_{0.52}Sb_{0.48}O_2$	P2	573	1.6	4
$K_{0.70}Zn_{0.35}Sn_{0.65}O_2$	P2	500	0.79	3

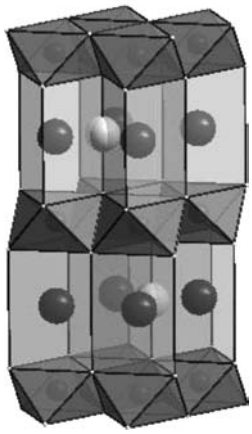

Figure 1. Polyhedral model of P2-phase structure $K_x(M_ySn_{1-y})O_2$. Dark octahedra represent $Sn(M)O_6$; transparent prisms represent KO_6 (for nonsplitted positions; K1 and K2 are shown as differently colored spheres).

The space group of more frequent O3 structure type is $R\bar{3}m$. This variety is not conventional for substances with interlayer K ions, but it is the most common for sodium compounds.

The space group of P3 structure type is also $R\bar{3}m$. Cations between layers fill trigonal prisms that share rectangular faces with each other. One half of these prisms has skeleton MO_6 octahedron at the top and a tetrahedral cavity at the bottom, and the other half has the opposite surroundings.

The space group for P2 structure type is $P6_3/mmc$. Cations between brucite-like layers are distributed over two types of trigonal prisms that share rectangular faces. One half of these prisms has adjacent edges with six octahedra from two nearest brucite-like layers, and the other half shares opposite faces with two octahedra. The compound $K_{0.72}In_{0.72}Sn_{0.28}O_2$ has this structure (Figure 1) and the highest potassium-ionic conductivity: 2.2 S/m at 500 K (on ceramics with a density of 85%).[5] Recently, a high ionic conductivity has been found in isostructural $K_{0.56}Ni_{0.52}Sb_{0.48}O_2$: 1.6 S/m at 573 K.[4]

Structures with prismatic coordination of interlayer cation reveal higher ionic mobility than structures with octahedral coordination of the same ions. It is explained by wider conductivity pathways and a larger number of available positions for moveable cations.[7]

The earlier solid electrolytes with high K^+-cation conductivity and general formula $K_xZn_{x/2}Sn_{1-x/2}O_2$ were first studied in ref 3. Hexagonal P2 phase is homogeneous at $0.70 \le x \le 0.80$. Zn and Sn cations occupy oxygen octahedra at random. These octahedra share edges to form brucite-like $(Zn,Sn)O_{6/3}$ layers.

Received: September 6, 2011
Published: April 11, 2012

Here, we present the results of investigation of phase formation in the $K_2O-Li_2O-SnO_2$ system, the structure and properties of novel solid electrolyte potassium lithiostannate, and a new technique for the synthesis of its zinc analogue.

2. EXPERIMENTAL SECTION

2.1. Synthesis and X-ray Diffraction Experiment. Samples of potassium zincostannate with P2 structure in the original work[3] were synthesized in two ways:

Table 2. Lattice Constants of Potassium Metallostannates with P2 Structure Type

compound	a [Å]	c [Å]	ref
$K_{0.70}(Zn_{0.35}Sn_{0.65}O_2)$	3.13	12.68	3
$K_{0.72}(In_{0.72}Sn_{0.26}O_2)$	3.2314	12.820	5
$K_{0.70}(Zn_{0.35}Sn_{0.65}O_2)$	3.14	12.68	this work
$K_{0.72}(Li_{0.24}Sn_{0.76}O_2)$	3.099	12.57	this work

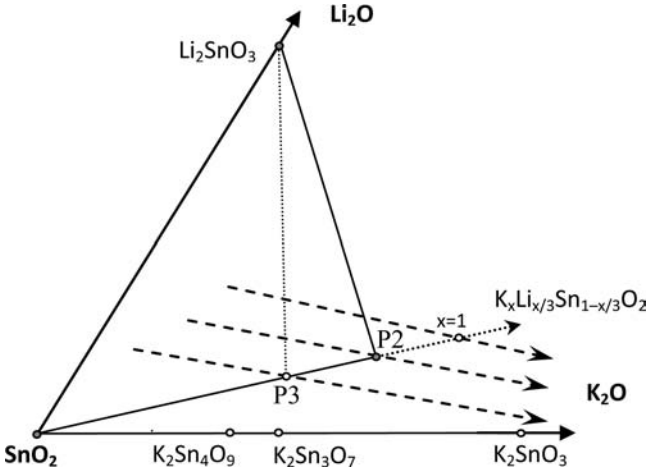

Figure 2. New phases in the system $K_2O-Li_2O-SnO_2$. Dashed arrows show the composition evolution with excess or loss of potassium oxide. Empty circles denote unstable or not existing compounds.

- by heating the K_2O, ZnO, and SnO_2 powders in soldered gold ampules at 1000 °C; and
- in two stages with the replacement of K_2O by KOH: for 15 h at 750 °C in oxygen current and for 15 h at 1000 °C in soldered gold ampules.

We developed a new synthesis technique for this class of materials. It is less expensive and easier, and it was tested for the above-mentioned compound.

The starting materials were Li_2CO_3, SnO_2, ZnO, and KOH (of analytical grade). Tin oxide and zinc oxide were being held for 4 h at 600 °C. Lithium carbonate was being dried at 200 °C for 2 h.

A series of simple potassium stannates is described in ref 8. We planned to use one of them as a precursor for potassium metallostannates. We tried to prepare $K_2Sn_3O_7$ from SnO_2 and KOH by two-stage heating: at 600 °C for 0.5 h and then at 800 °C for 2.5 h. However, we did not obtain any of the stannates in the product, even as an impurity. So the KOH was only used in subsequent syntheses as a potassium source.

Two other stannates were really used as intermediate forms. The lithium stannate has been obtained from Li_2CO_3 and SnO_2 by two steps. First, the components were ground, pressed, and calcined for 2 h at 700 °C. Then, after regrinding and pressing, the sample was newly heated for 2 h at 900 °C in air. Zn_2SnO_4 has been prepared from ZnO and SnO_2 by heating at 1000 °C for 6 h.

Table 3. List of Compositions $K_xLi_{x/3}Sn_{1-x/3}O_2$

No.	x	temperature of second stage [°C]	duration of second stage [h]	excess of KOH [%]	phases (X-ray data)
1	0.5	600	2	25	P2 + SnO_2 + Li_2SnO_3
2	0.6	600	2	25	P2 + SnO_2 + Li_2SnO_3
3	0.7	600 → 700	2 → 1	25	P2 + SnO_2
4	0.8	600	2	25	P2 + SnO_2 + Li_2SnO_3
5	0.9	600	2	25	P2 + SnO_2 + Li_2SnO_3
6	0.7	700	1.5	25	P2 + SnO_2 + Li_2SnO_3
7	0.7	700	2	25	P2 + SnO_2 + Li_2SnO_3
8	0.7	700	2.5	25	P2 + SnO_2 + Li_2SnO_3
9	0.7	1000	2	25	P2 + P3 + Li_2SnO_3
10	0.8	1000	2	25	P2+ Li_2SnO_3
11	0.9	1000	2	25	P2 + Li_2SnO_3
12	0.72	1000	2	50	P2 + Li_2SnO_3
13	0.72	1000	2	100	P2 + Li_2SnO_3
14	0.72	1000	2	150	P2
15	1	1100	2	25	P2 + Li_2SnO_3

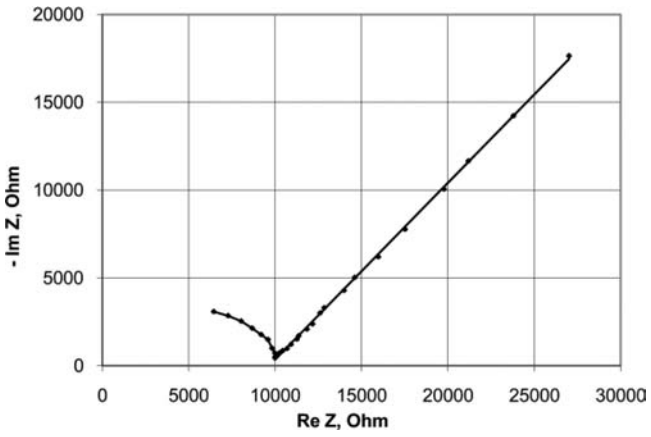

Figure 3. Impedance plot of $K_{0.72}Li_{0.24}Sn_{0.76}O_2$ (473 K).

X-ray diffraction (XRD) patterns were obtained on a ARL'Xtra diffractometer using monochromatized Cu Kα radiation. For profile preparing, the instant coffee powder was admixed to all samples to reduce grain orientation effect. The corundum powder [National Institute of Standards and Technology (NIST) Standard Reference Material (SRM) 676, available from International Centre for Diffraction Data (ICDD)] was used as an internal standard.

The compound $K_{0.70}Zn_{0.35}Sn_{0.65}O_2$ was synthesized from KOH (with 25% excess), SnO_2, and Zn_2SnO_4 in two stages. At the first stage, the initial substances were being held at 600 °C for 30 min. During this stage, the KOH melted down and impregnated two other powders. Then, the substances were ground, pressed into the pellet, and heated in a corundum crucible with a slow temperature increase up to 1100 °C in order to remove gaseous interaction products. The reaction mass then was held at 1100 °C for 2 h. The obtained specimens were identified by powder XRD method and appeared to be a pure P2 phase (Table 2), as in ICDD Card No. 00-35-1022.[9]

dx.doi.org/10.1021/ic201952x | Inorg. Chem. 2012, 51, 4931−4937

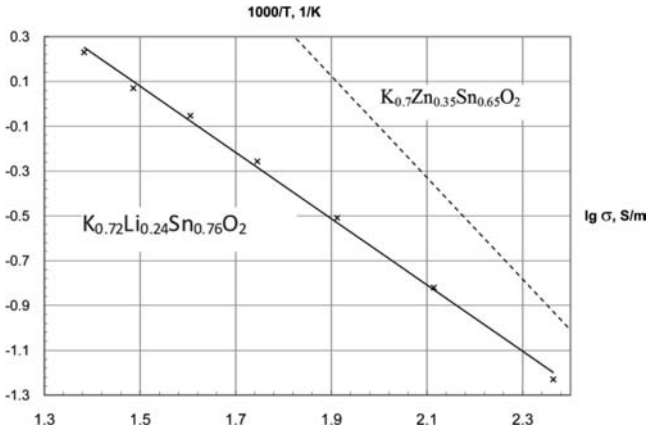

Figure 4. Temperature dependence followed the equation $\log \sigma = f(1/T)$. Solid line represents $K_{0.72}Li_{0.24}Sn_{0.76}O_2$, and the dashed line represents $K_{0.70}Zn_{0.35}Sn_{0.65}O_2$.[3]

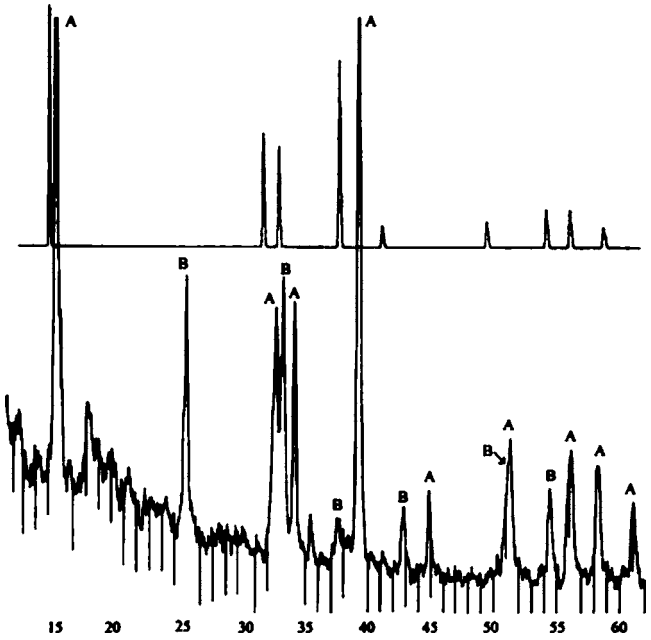

Figure 5. Powder XRD pattern of calcined $Na_{0.72}Li_{0.24}Sn_{0.76}O_2$. Top plot shows the spectrum for Na_2SnO_3 (modeling based on ICDD Card No. 00-35-1252);[9] bottom plot shows the experimental pattern with a lines of (A) a solid solution based on Na_2SnO_3 and (B) SnO_2 (ICDD Card No. 00-41-1445).[9]

Therefore, the new technique showed it to be successful and we used it for the next syntheses.

We investigated a set of compositions with general formula $K_xLi_{x/3}Sn_{1-x/3}O_2$ for the first time (Figure 2). They were synthesized from KOH, SnO_2, and Li_2SnO_3 in two stages, similar to the zinc analogue. We varied the x values, the excess of KOH, the temperature, and the duration of the second stage (Table 3). The obtained specimens were analyzed by powder XRD. The only crystalline phase P2 of a new potassium lithiostannate exists after heating at 1000 °C for 2 h (x = 0.72) with 150% excess of potassium hydroxide.

The need for such a big excess of KOH can be explained by the high activity of KOH used as one of the starting materials. At high temperatures, it interacts with carbon dioxide of the ambient air.

In order to make dense ceramics, we have changed conditions of the synthesis. Only the second stage (with longer duration and higher temperature) was first accomplished in the controllable atmosphere without water and carbon dioxide. So, the air flow passed through the concentrated sulfuric acid and then through the granulated sodium hydroxide. We also varied the temperature of the second stage from 900 °C up to 1050 °C. Then, both stages were carried out in this way and pure phases $K_{0.70}Zn_{0.35}Sn_{0.65}O_2$ and $K_{0.72}Li_{0.24}Sn_{0.76}O_2$ have been obtained at 1000 °C. The new technique of synthesis enabled us to prepare dense ceramics and, therefore, to measure the ionic conductivity of materials.

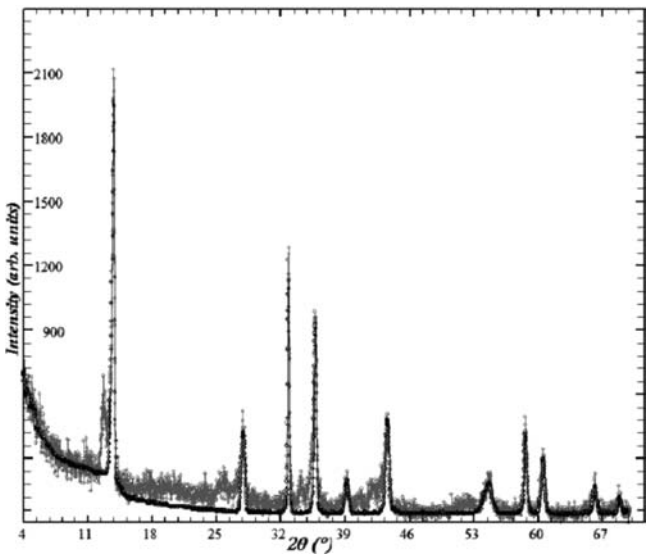

Figure 6. Powder XRD pattern of $K_{0.72}Li_{0.24}Sn_{0.76}O_2$. Black plot represents the freshly prepared sample, and the gray plot represents the material after hydrolysis.

Table 4. Details of Rietveld Refinement for $K_{0.72}Li_{0.24}Sn_{0.76}O_2$ at 298 K

		Agreement Factors	
parameter	value	parameter	value
space group	$P6_3/mmc$ (194)		
lattice constants			
a	3.09884(16) Å	R (obs)	1.78%
c	12.566(2) Å	R_w(obs)	2.27%
cell volume	104.50(2) Å^3	R (all)	1.84%
formula weight	153.09	R_w (all)	2.28%
wavelength	1.5406 Å	GOF	1.00
2Θ range	4°−70°	R_p	5.84%
step width	0.02°	R_{wp}	8.63%

The pattern of $K_{0.72}Li_{0.24}Sn_{0.76}O_2$ composition is similar to that of previously described $K_{0.70}Zn_{0.35}Sn_{0.65}O_2$ according to average ionic radii of Li/Sn and Zn/Sn mixtures.[12,13] As it is evident from Table 3, the homogeneity range is very narrow. Pure P2 phase exists only at x = 0.72.

When the x values decrease, the P3 phase appears (sample 9, Table 3); its lattice constants are a = 3.14 Å and c = 19.02 Å (compared to a = 3.120 Å and c = 19.03 Å for $K_{0.58}Zn_{0.29}Sn_{0.71}O_2$[3] of P3 type). However, we were not able to provide this phase in a pure state. As in ref 3, the results of its synthesis are poorly reproducible and the P3 phase seems to be metastable. All X-ray data show that only the SnO_2−Li_2SnO_3, SnO_2−P2, and P2−Li_2SnO_3 joins are stable at 1000−1000 °C (see Figure 2).

2.2. Properties of $K_{0.72}Li_{0.24}Sn_{0.76}O_2$. Cation mobility in $K_{0.72}Li_{0.24}Sn_{0.76}O_2$ was demonstrated by ion exchange and ion conductivity measurements in the frequency range from 8 Hz to 60 kHz. We used the controllable atmosphere for these purposes again, as described previously. Blocking graphite electrodes were applied. Complex impedance plots recorded at different temperatures (423−723 K) were analyzed to extract the bulk resistance. A typical plot is presented in Figure 3. Conductivity of 84% dense ceramics at 500 K is

dx.doi.org/10.1021/ic201952x | Inorg. Chem. 2012, 51, 4931−4937

Table 5. Atomic Coordinates and Displacement Parameters for $K_{0.72}Li_{0.24}Sn_{0.76}O_2$

position (site)	x/a	y/b	z/c	occup.	displacement parameters	
Sn (2a)	0	0	0	0.75(9)	U11	0.012(4)
					U22	0.012(4)
					U33	0.072(7)
					U12	0.0059(18)
K1 (4e)	0	0	0.210(15)	0.172(2)	U11	0.073(8)
					U22	0.073(8)
					U33	0.01(4)
					U12	0.037(4)
K2 (6 h)	0.25(5)	0.50(11)	3/4	0.150(6)	U11	0.09(3)
					U22	0.11(8)
					U33	0.02(3)
					U12	0.06(4)
O (4f)	1/3	2/3	0.072(3)	1	Uiso	0.0724(18)
Li (2a)	0	0	0	0.2(3)		0.1(2)

Table 6. Selected Interatomic Distances and Valence Angles in $K_{0.72}Li_{0.24}Sn_{0.76}O_2$

		Ionic Radii Sum [Å]			
atom pair	interatomic distance [Å]	from ref 12	from ref 13	valence angle [°]	
Sn−O	2.0071	0.83 + 1.24 = 2.07	0.71 + 1.40 = 2.11	O−Sn(Li)−O	6 × 78.943
Sn−O	2.0071	0.83 + 1.24 = 2.07	0.71 + 1.40 = 2.11		6 × 101.057
Li−O	2.0071	0.90 + 1.24 = 2.14	0.68 + 1.40 = 2.08	O−K−O (from centers of prisms)	3 × 102.562
Li−O	2.0071	0.90 + 1.24 = 2.14	0.68 + 1.40 = 2.08		6 × 65.599
K−O	2.8604 (from centers of prisms)	1.52 + 1.24 = 2.76	1.33 + 1.40 = 2.73		
K−O	K1: (3 × 2.4843, 3 × 3.2721)	1.52 + 1.24 = 2.76	1.33 + 1.40 = 2.73		
K−O	K2: (4 × 2.7535, 2 × 3.1586)	1.52 + 1.24 = 2.76	1.33 + 1.40 = 2.73		

0.23 S/m. Temperature dependence of conductivity is shown in Figure 4.

In the ion-exchange process, the potassium was replaced by sodium. Thoroughly dried $NaNO_3$ (with 30% excess) was admixed to $K_{0.72}Li_{0.24}Sn_{0.76}O_2$. These substances were ground together, pressed into a pellet, and held at 250 °C for 12 h. Powder XRD showed that the original structure type remained the same. The lattice constants of the obtained phase were a = 3.12 and c = 11.32 Å. Parameter c is similar to isostructural $Na_{0.6}Cr_{0.6}Ti_{0.4}O_2$ (a = 2.97, c = 11.24 Å)[7] and $Na_{0.68}Ni_{0.34}Ti_{0.66}O_2$ (a = 2.965, c = 11.16 Å)[10] with sodium between the layers. Therefore, we suppose that K ions have been completely replaced with Na ions. Parameter a increases from sodium metallotitanates to $Na_{0.72}Li_{0.24}Sn_{0.76}O_2$, in full compliance with a greater average ionic radius of Sn/Li, compared to Ti/Cr or Ti/Ni. Unfortunately, the samples dissolve neither in acids (nitric, sulfuric, and hydrochloric) nor in alkali. Therefore, we were unable to analyze them via atomic adsorption spectroscopy.

The $Na_{0.72}Li_{0.24}Sn_{0.76}O_2$ sample then was calcined for 2.5 h at 900 °C. According to X-ray data, it is decomposed into tin oxide and solid solution based on sodium stannate. The lattice constants of this solid solution are smaller than lattice constants of pure sodium stannate (Figure 5). Therefore, this means that lithium seems to be a constituent in the solid solution. The absence of P2 phase and any other potassium-containing phase after the latest calcination also provides evidence of the complete ion exchange.

2.3. Structure Refinement. The obtained sample of $K_{0.72}Li_{0.24}Sn_{0.76}O_2$ is rather hygroscopic and hydrolyzes very fast. Therefore, it must be stored in a dry desiccator with alkali. Figure 6 shows the powder XRD pattern of the freshly obtained sample and after exposure during 1 h in the air. Thus, there was no way to carry out slow scanning and the scanning rate was augmented to 4°/min.

Hexagonal parameters of $K_{0.72}Li_{0.24}Sn_{0.76}O_2$ were specified with an internal standard (corundum powder). As a starting model, we used the atomic coordinates of isostructural indiostannate $K_{0.72}In_{0.72}Sn_{0.28}O_2$.[5]

The space group for new compound is $P6_3/mmc$. A potassium indiostannate was first described in space group $P\bar{6}m2$. However, later, the correct space group was proposed for this family[10] and it was used in the next papers.[4,11]

To fit the structure, we applied the JANA2000 package. The structure refinement was carried out with the damping factor of 0.01. Thirty six (36) terms of Chebyshev polynoms were used to describe the background. We applied the Berar and Baldinozzi method for asymmetry correction and pseudo-Voigt profile function. We also took into account the preferred orientation, with respect to the 001 axis, according to March and Dollase. The results of refinement are shown in Tables 4−6. Calculated and observed powder XRD patterns are shown in Figure 7. Estimated standard deviations (ESDs) of displacement parameters are rather high. We believe that it is due to the low quality of the experimental pattern. However, the positive feature of refinement is the similarity of occupations sum and the starting chemical composition.

At the early stages of refinement, we obtained an extremely large value of the U33 parameter of K1 (0.21). It means that K1 is statically shifted or strongly oscillates along the z-axis. Therefore, we have changed the site type of K1 for 4e (it was 2b). We then refined the z-coordinate and have proved that K1 is really shifted from the center of the prism because of the alteration of skeleton neighbors (Li−Sn opposite to Sn−Sn or Li−Li cases). It is possible that the K ions are shifted to Li.

Similarly, U33 for K2 was decreased up to zero; the rather big ratio of U11 and U33 parameters showed that K2 is shifted or oscillates in the xy-plane. We also have changed site type of K2 for 6 h (it was 2d). Its x and y coordinates then were refined. K ions are shifted to the rectangular faces of prisms because of the high ionic conductivity in this plane. The electron density maps and arrangement of splitted K positions are shown in Figures 8 and 9.

dx.doi.org/10.1021/ic201952x | Inorg. Chem. 2012, 51, 4931−4937

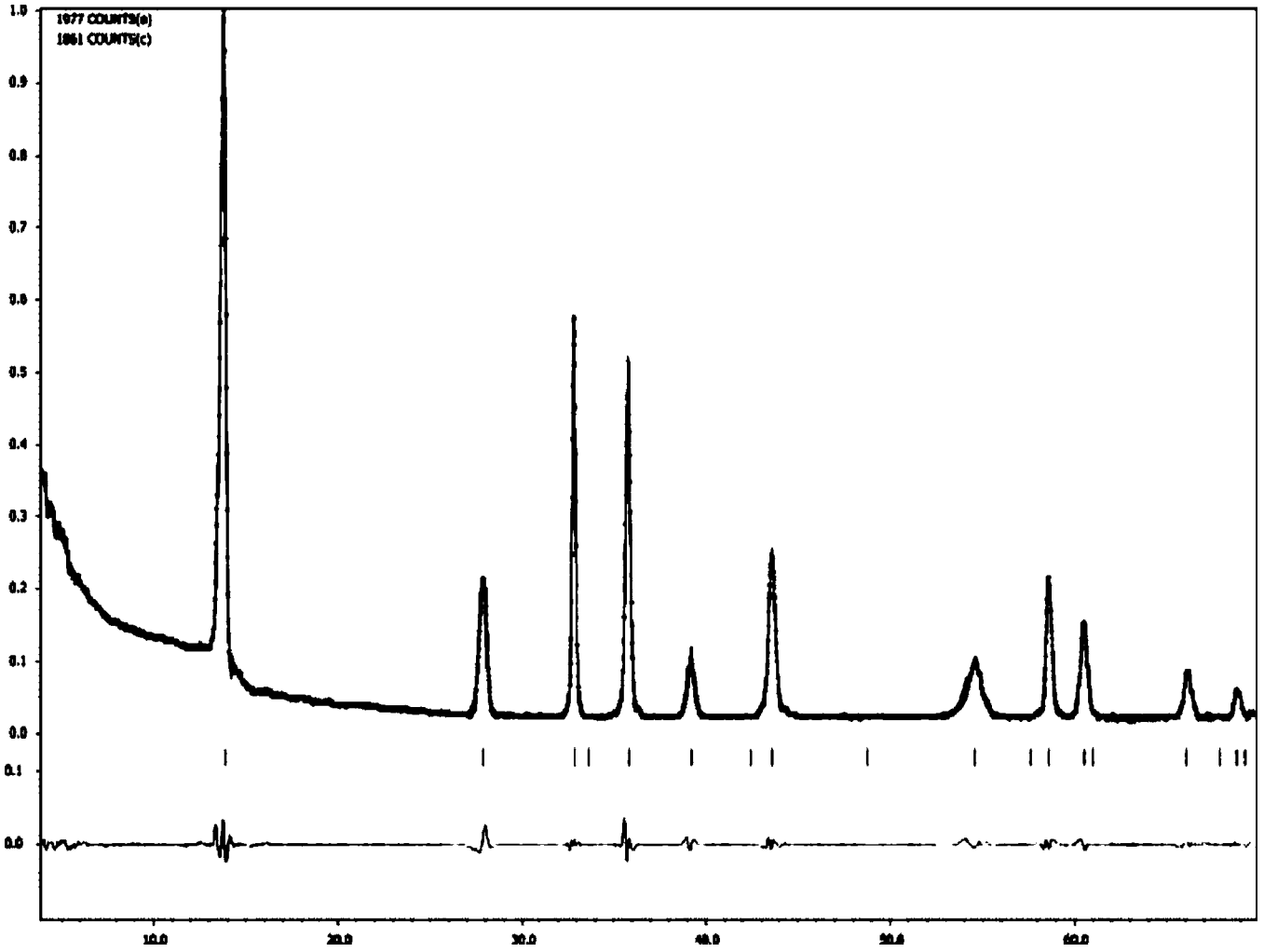

Figure 7. Calculated and observed powder XRD patterns of $K_{0.72}Li_{0.24}Sn_{0.76}O_2$. The difference (observed vs calculated) is plotted below. The short vertical bars indicate the Bragg positions of the reflections.

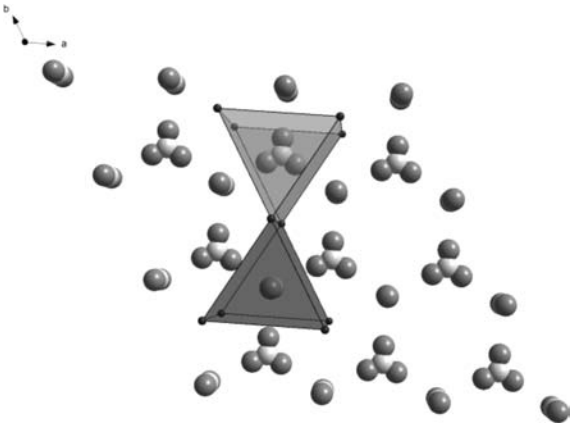

Figure 8. Splitted potassium positions (one layer). Light-colored spheres represent the centers of the prisms (two of them are shown); K1 positions are doubled, and K2 positions are tripled.

3. RESULTS AND DISCUSSION

Refinement results show that $Sn(Li)O_6$ octahedra are flattened along the 001 translation. This distortion reduces the repulsion between large K cations (see Figure 1).

The K−O interatomic distances (see Table 6) are extremely large, compared to the ionic radii sum, and the Sn/Li−O distances are extremely small. This information possibly shows that the *z*-coordinate of O is not determined correctly. If we use 0.082 instead of 0.072 (see Table 5), the K−O distances are 2.76 Å and the Sn/Li−O distances are 2.06 Å.

In our earlier model, Li atoms were neglected, because of their small X-ray scattering factors, compared to that of other atoms. It is very difficult to localize Li atoms using X-ray data. However, their position indirectly results from P2-phase lattice constants. Parameter *c* is similar to isostructural $K_{0.70}Zn_{0.35}Sn_{0.65}O_2$ with only potassium between the layers. For Li ions, prismatic coordination is not typical at all. Because of the small Li radius, prism oxygen ions are located too close to each other. In addition, the distance between layers is too large for lithium. Therefore, Sn and Li cations occupy oxygen octahedra at random.

Moreover, as claimed previously, when we tried to obtain potassium stannates, the similar technique of synthesis and the same SnO_2 and KOH starting materials were used, but without Li_2SnO_3. Consequently, we did not obtain P2 or P3 phase. Thus, we have decided that the P2 and P3 phases do not exist without lithium. At the final stage of structure refinement, Li positions have been included in the model.

dx.doi.org/10.1021/ic201952x | *Inorg. Chem.* 2012, 51, 4931−4937

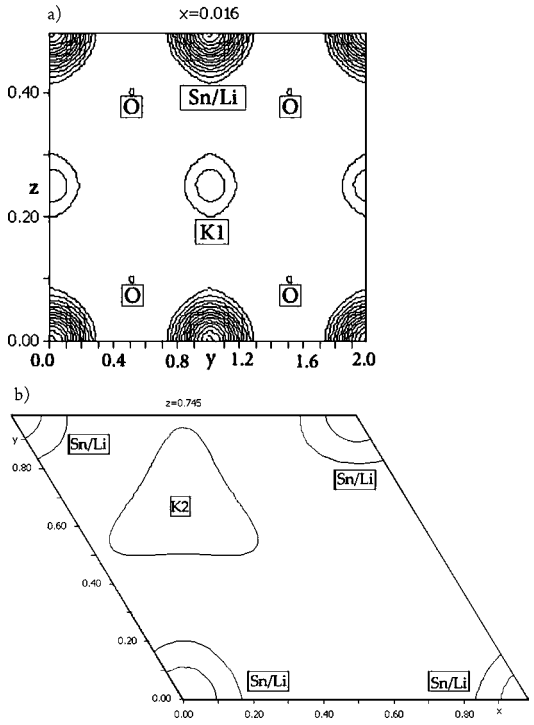

Figure 9. Electron density maps in $K_{0.72}Li_{0.24}Sn_{0.76}O_2$: (a) in the plane with constant x value and (b) in the plane normal to the z-axis.

Table 7. Some Complex Oxometallates $A_xB_yC_{1-y}O_2$ with Brucite-Like Layers

$A_xB_yC_{1-y}O_2$ (structure type)	R(A)/R(B)	R(B)/R(C)	ΔEN (C−B)	ΔEN (B−A)	ref
$Na_{0.8}Fe_{0.8}Ti_{0.2}O_2$ (O3)	1.48	1.05	−0.29	0.90	1
$Na_{0.68}Mg_{0.68}Ti_{0.32}O_2$ (O3)	1.35	1.15	0.23	0.38	2
$K_{0.58}Zn_{0.29}Sn_{0.71}O_2$ (P3)	1.73	1.06	0.31	0.83	3
$K_{0.59}Mg_{0.53}Sb_{0.47}O_2$ (P3)	1.77	1.16	0.74	0.49	4
$K_{0.72}In_{0.72}Sn_{0.28}O_2$ (P2)	1.62	1.13	0.18	0.96	5
$K_{0.56}Ni_{0.52}Sb_{0.48}O_2$ (P2)	1.83	1.12	0.14	1.09	4
$K_{0.7}Zn_{0.35}Sn_{0.65}O_2$ (P2)	1.73	1.06	0.31	0.83	3
$LiCo_{0.6}Fe_{0.4}O_2$ (O3)	1.14	1.01	−0.05	0.90	14
$Na_{0.67}Ni_{0.33}Mn_{0.67}O_2$ (P2)	1.34	1.24	−0.36	0.98	15
$Na_{0.6}Al_{0.12}Mn_{0.88}O_2$ (P3)	1.72	1.01	−0.06	0.68	16
$Na_{0.67}Mn_{0.83}Li_{0.17}O_2$ (P2)	1.73	0.74	−0.57	0.62	17
$Na_{0.67}Mn_{0.97}Cr_{0.03}O_2$ (P2)	1.73	0.89	0.11	0.62	17
$Na_{0.67}Mn_{0.9}Mg_{0.1}O_2$ (P2)	1.73	0.78	−0.24	0.62	17
$K_{0.72}Li_{0.24}Sn_{0.76}O_2$ (P2)	1.69	1.08	0.98	0.16	this work

The formula sum according to the refinement results is $K_{0.794}(Li_{0.2}Sn_{0.75})O_2$. It is electroneutral but deviates slightly from the composition determined using phase analysis data. It is not surprising, taking into account the poor quality of the X-ray profile.

The examples of phases with brucite-like layers (general formula: $A_xB_yC_{1-y}O_2$) are shown in Table 7. The B ion can occupy part of the C ion positions in the framework or part of the A ion positions between layers. In order to predict B ion positioning, it is necessary to compare the radii and electronegativities of A/B and C/B ions. In all examples in Table 7 (except two of them), these factors match each other. However, in case of $K_{0.59}Mg_{0.53}Sb_{0.47}O_2$ and $K_{0.72}Li_{0.24}Sn_{0.76}O_2$, these parameters compete with each other: the electronegativities of the B ions (Mg, Li) are similar to that of the A ion (K), but their radii are comparable to that of the C ions (Sb, Sn). We see, that the geometrical similarity is more important: the same variant of arrangement is realized in all substances, i.e., B ions (Mg, Li) are mixed up only with C ions (Sb, Sn). Therefore, in the new P2 and P3 phases, lithium is a skeleton cation; it is included in brucite-like layers and has "acid" properties.

■ ASSOCIATED CONTENT

Ⓢ Supporting Information

This material is available free of charge via the Internet at http://pubs.acs.org.

■ AUTHOR INFORMATION

Corresponding Author

*E-mail: ishukaev@sfedu.ru.

Notes

The authors declare no competing financial interest.

■ ACKNOWLEDGMENTS

We are grateful to the reviewers for helpful discussion and useful suggestions that significantly improved the manuscript. We also are thankful to M. Sorokina for working on the text.

■ REFERENCES

(1) Li, C.; Reid, A. F.; Saunders, S. *J. Solid State Chem.* **1971**, *3*, 614.
(2) Nalbandyan, V.; Rykalova, S.; Bikyashev, E. *Zh. Neorg. Khim.* **1989**, *34*, 1356 (in Russ.).
(3) Maazaz, A.; Delmas, C.; Fouassier, C.; Reau, J.-M.; Hagenmuller, P. *Mater. Res. Bull.* **1979**, *14*, 193.
(4) Smirnova, O.; Nalbandyan, V.; Avdeev, M.; Medvedeva, L. I.; Medvedev, B. S.; Kharton, V. V.; Marques, F. M. B. *J. Solid State Chem.* **2005**, *178* (1), 172.
(5) Delmas, C.; Werner, P.-E. *Acta Chem. Scand., A* **1978**, *A32*, 329.
(6) Delmas, C.; Fouassier, C.; Hagenmuller, P. *Mater. Res. Bull.* **1976**, *11*, 1081.
(7) Avdeev, M.; Nalbandyan, V. B.; Shukaev, I. L. Cation and proton conductors: relationships between composition, crystal structure, and properties. In *Solid State Electrochemistry I: Fundamentals, Methodology and Applications*; Kharton, V. V., Ed.; Wiley−VCH, Weinheim, Germany, 2009; pp 227−278.
(8) Delmas, C.; Demazeau, G. *J. Solid State Chem.* **1976**, *19*, 87.
(9) International Centre for Diffraction Data (ICDD). *ICDD Powder Diffraction Data File*, Release 2008.
(10) Nalbandyan, V. B.; Shukaev, I. L. *Zh. Neorg. Khim.* **1992**, *37* (11), 2387−2394 (in Russ.).
(11) Smirnova, O. A.; Shukaev, I. L.; Medvedev, B. S. Crystal chemistry and cation transport properties of mixed sodium or potassium antimonates. In *Solid State Chemistry 2000, Book of Abstracts*; Bezdicka, P.; Grygar, T., Eds.; Sept. 3−8, 2000, Prague, Czech Republic; p 228.
(12) Shannon, R. D. *Acta Crystallogr., Sect. A: Cryst. Phys., Diffr. Theor. Gen. Crystallogr.* **1976**, *32A*, 751.
(13) Ahrens, L. H. *Geochim. Cosmochim.* **1952**, *2A*, 155.
(14) Chappel, E.; Holzapfel, M.; Chouteau, G.; Ott, A. *J. Solid State Chem.* **2000**, *154*, 451.
(15) Matsumura, T.; Sonoyama, N.; Kanno, R. *Solid State Ionics* **2003**, *161*, 31.

(16) Patoux, S.; Dolle, M.; Doeff, M. M. *Chem. Mater.* **2005**, *17*, 1044.
(17) Wei, M.; Lu, Y.; Evans, D. G.; Duan, X. *Solid State Ionics* **2003**, *161*, 133.